chemistry

MDPI

Communication

Pentacoordinate Carbon Atoms in a Ferrocene Dication Derivative—$[Fe(Si_2\text{-}\eta^5\text{-}C_5H_2)_2]^{2+}$

Shilpa Shajan [1], Jin-Chang Guo [2], Aland Sinjari [3], Krishnan Thirumoorthy [1] and Venkatesan S. Thimmakondu [4,*]

1 School of Advanced Sciences, Vellore Institute of Technology, Vellore 632 014, Tamil Nadu, India
2 Nanocluster Laboratory, Institute of Molecular Science, Shanxi University, Taiyuan 030006, China
3 School of Mathematics, Biological, Exercise & Physical Sciences, San Diego Miramar College, San Diego, CA 92126-2910, USA
4 Department of Chemistry and Biochemistry, San Diego State University, San Diego, CA 92182-1030, USA
* Correspondence: vthimmakondusamy@sdsu.edu

Abstract: Pentacoordinate carbon atoms are theoretically predicted here in a ferrocene dication derivative in the eclipsed-(**1**; C_{2v}), gauche-(**2**; C_2) and staggered-$[Fe(Si_2\text{-}\eta^5\text{-}C_5H_2)_2]^{2+}$(**3**; C_{2h}) forms for the first time. Energetically, the relative energy gaps for **2** and **3** range from −3.06 to 16.74 and −2.78 to 40.34 kJ mol^{-1}, respectively, when compared to the singlet electronic state of **1** at different levels. The planar tetracoordinate carbon (ptC) atom in the ligand $Si_2C_5H_2$ becomes a pentacoordinate carbon upon complexation. The ligand with a ptC atom was predicted to be both a thermodynamically and kinetically stable molecule by some of us in our earlier theoretical works. Natural bond orbital and adaptive natural density partitioning analyses confirm the pentacoordinate nature of carbon in these three complexes (**1**–**3**). Although they are hypothetical at the moment, they support the idea of "hypercoordinate metallocenes" within organometallic chemistry. Moreover, ab initio molecular dynamics simulations carried out at 298 K temperature for 2000 fs suggest that these molecules are kinetically stable.

Keywords: ferrocene; hypercoordinated-metallocene; $[Fe(Si_2\text{-}\eta^5\text{-}C_5H_2)_2]^{2+}$; pentacoordinate carbon; planar tetracoordinate carbon; kinetic stability; DFT calculations

Citation: Shajan, S.; Guo, J.-C.; Sinjari, A.; Thirumoorthy, K.; Thimmakondu, V.S. Pentacoordinate Carbon Atoms in a Ferrocene Dication Derivative—$[Fe(Si_2\text{-}\eta^5\text{-}C_5H_2)_2]^{2+}$. *Chemistry* **2022**, *4*, 1092–1100. https://doi.org/10.3390/chemistry4040074

Academic Editor: Andrea Peluso

Received: 16 August 2022
Accepted: 19 September 2022
Published: 21 September 2022

1. Introduction

Ferrocene, $Fe(\eta^5\text{-}C_5H_5)_2$, is an important molecule that has been used over the last seven decades [1–4]. It opened a new avenue called organometallic chemistry, which has been continuously growing since 1951 [5–9]. Here, using $Si_2C_5H_2$ as a ligand instead of cyclopentadienyl anion ($C_5H_5^-$), three ferrocene derivative dication structures are theoretically identified—eclipsed-(**1**; C_{2v}), gauche-(**2**; C_2), and staggered-$[Fe(Si_2\text{-}\eta^5\text{-}C_5H_2)_2]^{2+}$(**3**; C_{2h})—that shows hypercoordinate nature (pentacoordination) to its one of the ligand carbon atoms (see Figure 1). Before complexation, the bare ligand contains a planar tetracoordinate carbon (ptC) atom [10–16]. In the last five decades, many molecules containing ptC atom have been theoretically predicted [17–30] because of the pioneering theoretical work of Hoffmann [10,31] and Schleyer [11,32], and some are experimentally realized [33–37]. All the structures (**1**–**3**) exhibit two pentacoordinate carbon atoms, each upon forming a complex with Fe^{2+}. Carbon showing hypercoordinate behavior—either penta or hexa—is rare but not very new to chemists [38–42]. Non-planar pentacoordination to carbon has already been well established in systems such as CH_5^+ [38,43], CLi_5 [44], $C(CH_3)_5^+$ [45], $[(Ph_3PAu)_5C]^+$ [46], and $Si_2(CH_3)_7^+$ [47]. Likewise, non-planar hexacoordination to carbon has been proven in CLi_6 [44,48], $[(Ph_3PAu)_6C]^{2+}$ [49], and $C_6(CH_3)_6^{2+}$ [50,51]. Carbon atom having heptacoordination is theoretically predicted in CH_7^{3+} [52], $[CTi_7]^{2+}$ [53], and also in trophylium trication, $C_7H_7^{3+}$ [54]. The octacoordination of carbon atom was also

theoretically established in carborane clusters [55] and CBe_8H_{12} [56]. Through $[Fe(Si_2\text{-}\eta^5\text{-}C_5H_2)_2]^{2+}$, our aim is to open a new avenue within organometallic chemistry called "hypercoordinated metallocenes containing five bonds to carbon" [57–60].

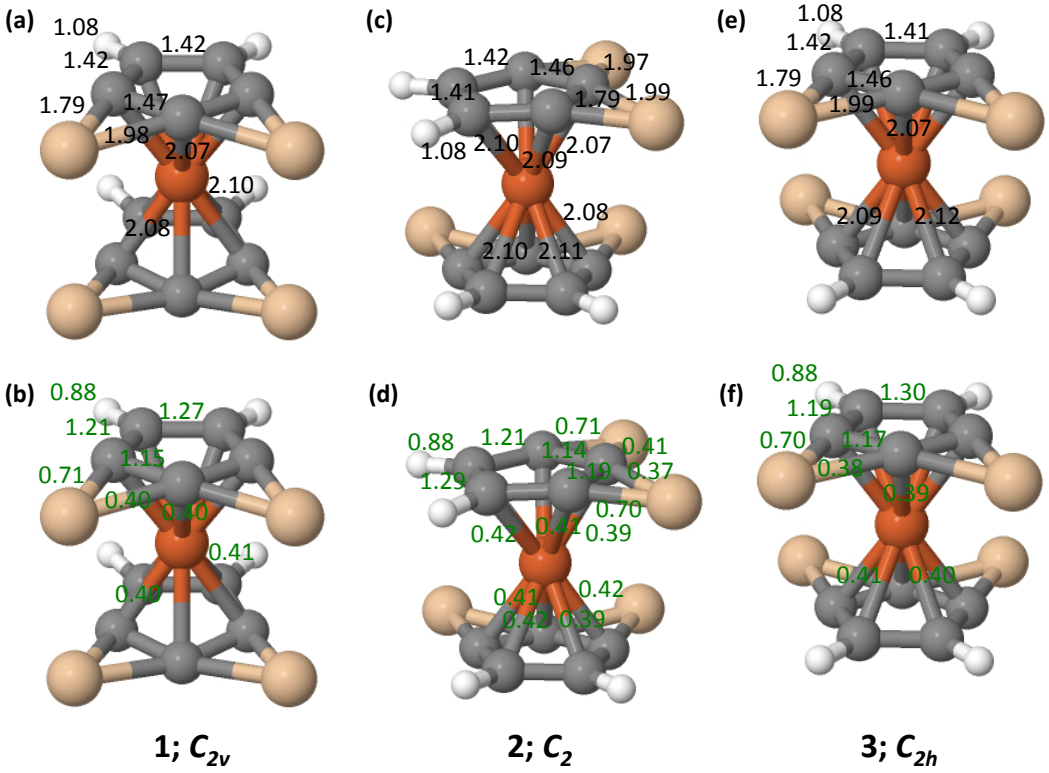

Figure 1. Optimized singlet electronic state structures of (**a**) eclipsed-, ($^1A_1$) (**c**) gauche-, (^1A) and (**e**) staggered-$[Fe(Si_2\text{-}\eta^5\text{-}C_5H_2)_2]^{2+}$ (^1A_g) (Fe:orange; Si:bisque; C:gray; H:white) obtained at the ωB97X-D/def2-TZVP level of theory. Bond lengths are indicated in Å. Wiberg bond indices (in green) calculated at the same level are given in (**b**), (**d**), and (**f**), respectively.

Various isomers of $Si_2C_5H_2$ have been theoretically identified by some of us in an earlier theoretical work and it was concluded that the molecule with a ptC atom, 2,7-disilatricyclo[4.1.0.$0^{1,3}$]hept-2,4,6-trien-2,7-diyl, is the most stable structure thermodynamically [27]. The global minimum geometry of $Si_2C_5H_2$ has been theoretically verified elsewhere through search algorithms [61]. The kinetic stability of the thermodynamically most stable isomer through appropriate dissociation pathways has been analyzed in detail recently [62]. It was proven theoretically that the global minimum isomer of $Si_2C_5H_2$ with a ptC atom is not only thermodynamically stable but also kinetically stable [62]. Thus, in this work, new complexes using $Si_2C_5H_2$ as a ligand with Fe(II) are theoretically characterized here. Optimized structures of eclipsed-, gauche-, and staggered-$[Fe(Si_2\text{-}\eta^5\text{-}C_5H_2)_2]^{2+}$ obtained at the ωB97X-D/def2-TZVP level of theory are shown in Figure 1a, 1c, and 1e, respectively. Like ferrocene, the oxidation state of Fe in all three different forms (**1**, **2**, and **3**) is +2 (i.e., Fe(II) [Ar] $3d^6$). However, the ligands ($Si_2C_5H_2$) are neutral here with 6π electrons each. Nevertheless, these complexes do attain the 18-electron configuration or to put it in simpler terms, they do follow the effective atomic number (EAN) rule (EAN = 36; 24 electrons from Fe(II) and 12 π electrons from the ligands) and attain the electron configuration of Kr.

2. Computational Details

All geometry optimization and frequency calculations were carried out using def2-TZVP basis sets [63]. Various density functionals were used such as B3LYP [64], TPSSh [65], M06-L [66], and ωB97X-D [67]. Calculations were also carried out with empirical dis-

persion corrections (D3) [68] with Becke–Johnson damping (BJ) [69,70] (i.e., B3LYP-D3BJ, TPSSh-D3BJ) to observe the geometrical changes due to dispersion (van der Waals) interactions. . Natural bond orbital analyses were conducted using ωB97X-D functional to obtain the natural atomic charges and Wiberg bond indices (WBIs) [71]. Ab initio molecular dynamics (AIMD) simulations using the atom-centered density matrix propagation (ADMP) [72] method were also carried out to check the kinetic stability of these complexes. All calculations were carried out using the Gaussian program package [73].

3. Results and Discussion

The zero-point vibrational energy (ZPVE) corrected-relative energies and Gibbs free energies obtained for **1–3** at different levels for the singlet and quintet electronic states are shown in Table 1. It is noted here that calculations were carried out for the triplet electronic states of these complexes. However, they turned out to be lying above singlets and quartets and thus for brevity they are given in the supporting information (see Table S3 for details). Bonding pattern obtained for eclipsed conformer (**1**) through AdNDP analysis is shown in Figure 2.

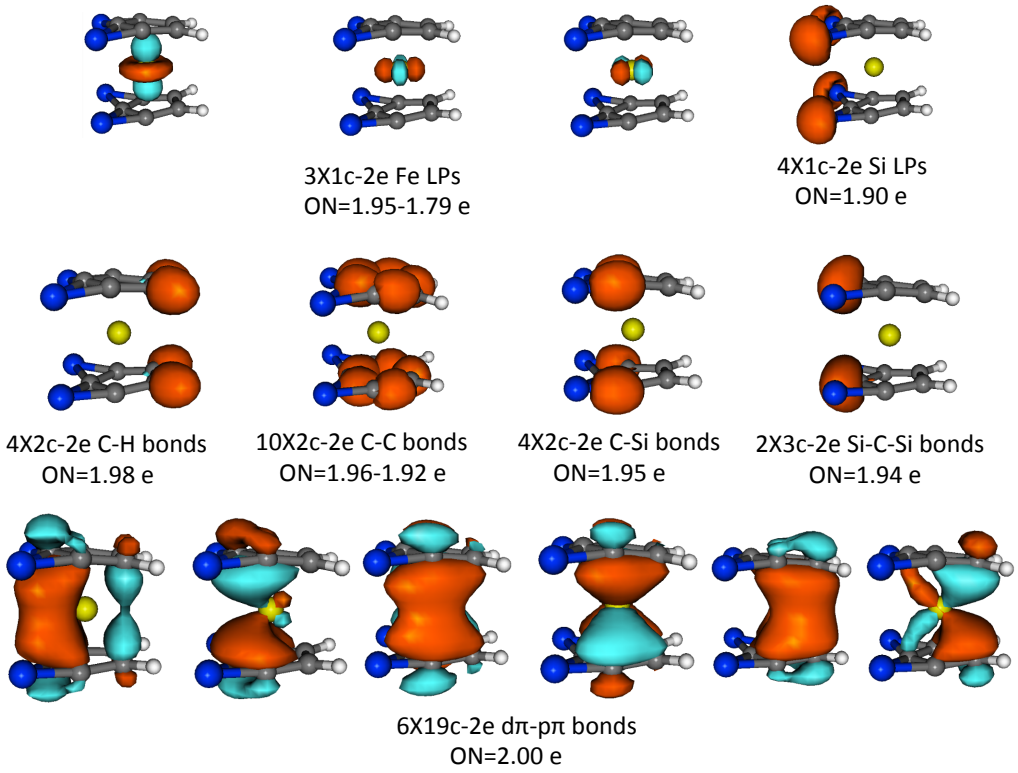

Figure 2. Chemical bonding pattern for eclipsed-$[Fe(Si_2\text{-}\eta^5\text{-}C_5H_2)_2]^{2+}$ (**1**) as obtained from AdNDP analysis. Lone-pairs (LPs), 2center-2electron (2c-2e), and various multicenter-2electron (3c-2e, 4c-2e, and 19c-2e) bonds including their occupation numbers (ONs) are shown.

Table 1. ZPVE-corrected relative energies (ΔE_0) and thermally corrected Gibbs energies ($\Delta G_{298.15}$) of **2** and **3** relative to the singlet electronic state of **1** ($^1A_1$) using def2-TZVP basis set [a].

	1 (Eclipsed)		**2 (Gauche)**				**3 (Staggered)**			
	Quintet [b]		**Singlet**		**Quintet**		**Singlet**		**Quintet**	
Functional	ΔE_0	$\Delta G_{298.15}$	ΔE_0	$\Delta G_{298.15}$	ΔE_0	$\Delta G_{298.15}$	ΔE_0	$\Delta G_{298.15}$	ΔE_0	$\Delta G_{298.15}$
B3LYP	−29.14	−39.04	−2.34	−3.16	−36.36	−51.01	−2.47	−4.59	−39.25	−54.01
B3LYP-D3BJ	−7.90	−19.59	2.44	1.38	−13.04	−30.40	8.24	5.51	−2.91	−22.72
M06-L	94.58	82.77	16.74	16.75	88.72	73.84	40.34	37.89	85.93	69.80
TPSSh	95.60	82.17	13.30	12.57	89.24	72.20	30.78	28.14	86.90	69.16
TPSSh-D3BJ	118.33	108.34	13.54	13.53	113.96	95.88	32.29	31.16	112.57	93.01
ωB97X-D	0.31	−4.17	−3.06	2.04	−5.11	−13.61	−2.78	−1.21	−7.82	−15.63

[a] All values are in kJ mol^{-1}. [b] Transition state or second-order saddle-point at this level.

3.1. Energetics

As far as relative stability is concerned among the three, different DFT functionals gave us different results (see Table 1). The quintet electronic state of the staggered (**3**) form is the most stable at the ωB97X-D/def2-TZVP level. However, with the same def2-TZVP basis set, functionals such as M06-L, TPSSh, and TPSSh-D3BJ predict that the singlet electronic state of the eclipsed form (**1**) is the most stable. With the popular functional B3LYP, though we obtain the quintet of **3** as the most stable, adding empirical dispersion corrections on top of B3LYP (i.e, B3LYP-D3BJ) changes the result yet again because at the B3LYP-D3BJ/def2-TZVP level, the quintet of gauche-form (**2**) is the most stable. Like ferrocene, the relative energy gap (∼4 kJ mol^{-1}) between staggered and eclipsed forms is quite small [8]. In the parent molecule, as per gas-phase calculations, the staggered form is a saddle-point (transition state) and the eclipsed form is a minimum [74]. In the derivatives studied here, all the three different forms in their singlet ground electronic state are minima at all levels. The quintet electronic states of staggered (**3**) and gauche (**2**) conformers are also minima whereas the eclipsed (**1**) conformer of quintet either turns out to be a transition-state or a second-order saddle-point at different levels. Our main motivation in this study is to analyze the bonding scenario and thus we leave this discussion with a caveat that various DFT functionals including the popular B3LYP underestimate the barrier-heights [75,76].

3.2. Bonding

Let us analyze the bonding scenario in these cations (**1**–**3**) as each isomer contains two pentacoordinate carbon atoms. The C-C bond length in **1** (C_{2v}) range from 1.42 to 1.47 Å (see Figure 1a), whereas in **2** (C_2) and **3** (C_{2h}) it varies from 1.41 to 1.46 Å (see Figure 1c,e). Compared to ferrocene [77], where the mean C-C bond length is equal to 1.431 Å, these bond lengths are slightly varied, which is reasonable due to the ionic character (dication) in these complexes apart from the presence of silicon atoms. Likewise, the Fe-C bond length in **1** range from 2.07 to 2.10 Å, whereas in **2** and **3** it varies from 2.07 to 2.11 Å and 2.07 to 2.12 Å, respectively. In ferrocene, the mean Fe-C bond length is equal to 2.059 Å and here they are slightly longer. The Si-C bond length connected to the pentacoordinate carbon is 1.98 Å in **1**, 1.97 and 1.99 Å in **2**, and 1.99 Å in **3**, which reflects its single bond characteristics whereas the Si-C bond on the sides are shorter with a bond length of 1.79 Å in all the three forms. In principle, the isolated $Si_2C_5H_2$ ligand almost behaves like a cyclopentadienyl anion ($C_5H_5^-$), with a slight exception that the former contains a 3center-2electron (3c-2e) σ bond (see Figure 2) around the Si-C-Si region [61,62]. This is evidently seen even when it makes complexation with Fe(II).

3.3. Wiberg Bond Indices

The presence of pentacoordinate carbon atoms could be further justified with the WBIs calculated for **1**, **2**, and **3**, in Figure 1b, 1d, and 1f, respectively. In all cases, the WBI values for Fe-C are in the range of 0.39 to 0.42. This indicates that they are indeed single bonds. The hypercoordinate C-Si WBI values in **1** and **3** are 0.40 and 0.38, respectively, whereas for **2** we obtained two values due to reduced symmetry and they are 0.37 and 0.41, respectively. All these values also reflect the single bond characteristics of these bonds. The Si-C WBI values in **1** to **3** are in the range of 0.71 to 0.70 showing single bond characteristics. WBI values for all C-C bond lengths are greater than one, which indicates resonance stabilization plus double bond characteristics. On the basis of these values, one could certainly conclude that the central carbon atoms are hypercoordinate (penta) in all the three forms. It is emphasized here that each hypercoordinate carbon obeys the octet-rule as the total WBI for each pentacoordinate carbon is 3.62 for **1** and **2**, whereas it is 3.61 for **3**. However, some of the bonds (Si-C and C-Fe) are electron-deficient bonds with fewer than two electrons as mentioned elsewhere in the example of $C(CH_3)_5^+$ [45].

3.4. AdNDP Analysis

To clarify the chemical bonding pattern further in these complexes, we carried out adaptive natural density partitioning (AdNDP) analysis [78,79] using the Multiwfn [80] program. For brevity, only the bonding patterns of the eclipsed conformer alone are shown here. In total, 66 valence electrons **1** are taken into account. Seven lone-pairs (LPs), four 2c-2e C-H bonds, ten 2c-2e C-C bonds, four 2c-2e C-Si bonds, two 3c-2e Si-C-Si σ bonds, and six 19c-2e $d\pi$-$p\pi$ are shown in Figure 2. Among them, the latter are more important as they support the pentacoordinate nature of the central carbon atom. Though **1**–**3** are hypothetical examples at the moment, theoretically, these complexes support the idea of "hypercoordinate metallocenes" within organometallic chemistry.

3.5. MD Simulations

To verify the kinetic stability of the ferrocene derivatives (**1**–**3**), we have carried out ab initio molecular dynamics simulations using ADMP method [72]. These simulations are done at 298 K temperature and 1 atm pressure for 2000 fs time. For brevity, the time evolution of total energy for the eclipsed isomer **1** computed at the ωB97XD/def2-TZVP level for 2000 fs time scale is shown in Figure 3. Similar plots for isomers **2** and **3** are shown in the supporting information. To clearly depict the alteration of the structure over the 2000 fs of time, snapshots at 400 fs interval have been added. Considering the low-energy gap among the three different forms, it is not surprising to see that the structure rotates quite freely and at the time of 1200 fs itself, one could notice a structure that is very close to the gauche-form (**2**). However, none of the structures broke altogether, which indicates that all these three different forms of $[Fe(Si_2\text{-}\eta^5\text{-}C_5H_2)_2]^{2+}$ are kinetically stable.

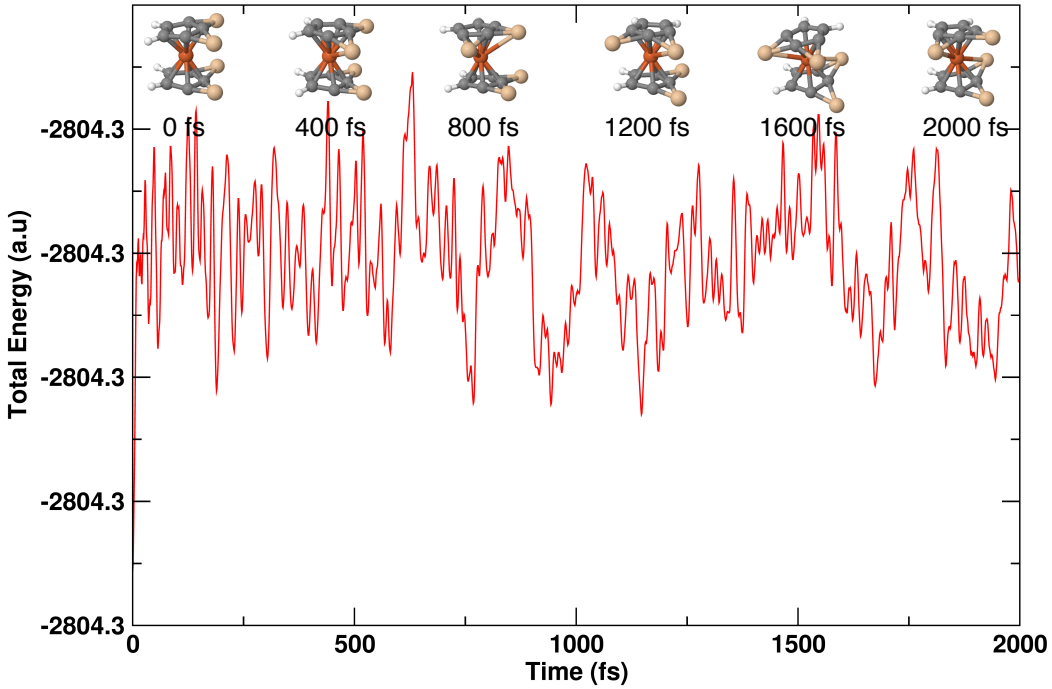

Figure 3. Time versus energy plot of isomer **1** of $[Fe(Si_2\text{-}\eta^5\text{-}C_5H_2)_2]^{2+}$ obtained from the AIMD simulation carried out at 298 K and 1 atm pressure for 2000 fs at the ωB97XD/def2-TZVP level.

4. Conclusions

In conclusion, three ferrocene derivatives (**1**–**3**) are theoretically identified here using DFT at different levels. All of them contain two pentacoordinate carbon atoms. NBO and AdNDP analyses confirm that they are indeed pentacoordinate carbons. Ab initio MD simulations carried out at 298 K temperature for 2000 fs assert that they are kinetically stable molecules. For each pentacoordinate carbon, one 3c-2e Si-C-Si σ-bond (total two for each molecule) and three 19c-2e $d\pi$-$p\pi$-bonds (total six for each molecule) exist and they follow the existing pattern of $(2\sigma + 6\pi)$-dual aromaticity, which is a well-established pattern in ptC and hypercoordinate carbon molecules. Since the ligand here ($Si_2C_5H_2$) contains a ptC atom before complexation, these results are surprising. Theoretically, this new class of molecules could be termed "hypercoordinate metallocenes".

Supplementary Materials: The following supporting information can be downloaded at: https://www.mdpi.com/article/10.3390/chemistry4040074/s1, Supplementary file S1: Supporting information for this paper.

Author Contributions: Conceptualization, V.S.T.; methodology, S.S., V.S.T. and J.-C.G.; software, S.S., K.T., A.S. and V.S.T.; validation, V.S.T. and J.-C.G.; formal analysis, V.S.T., S.S., K.T. and A.S.; investigation, S.S., J.-C.G., A.S. and V.S.T.; resources, K.T., J.-C.G. and V.S.T.; data curation, S.S. and V.S.T.; writing—original draft preparation, V.S.T.; writing—review and editing, V.S.T.; visualization, S.S., J.-C.G. and V.S.T.; supervision, V.S.T.; project administration, V.S.T. All authors have read and agreed to the published version of the manuscript.

Funding: This research work did not receive any specific grant from public or private funding agencies. However, computational support provided at the SDSU (for AS and VST) by DURIP Grant W911NF-10-1-0157 from the U.S. Department of Defense and by NSF CRIF 338 Grant CHE-0947087 is gratefully acknowledged.

Data Availability Statement: Data available in article or Supplementary Materials.

Acknowledgments: Additional computational support provided to SS and KT at VIT, Vellore, India, is also gratefully acknowledged. VST thanks Andrew L. Cooksy (SDSU, San Diego) for providing additional computing time.

Conflicts of Interest: The authors declare no conflict of interest.

Abbreviations

The following abbreviations are used in this manuscript:

ADMP	Atom-Centered Density Matrix Propagation
AIMD	Ab Initio Molecular Dynamics
AdNDP	Adaptive Natural Density Partitioning
DFT	Density functional theory
EAN	Effective Atomic Number
MD	Molecular Dynamics
NBO	Natural Bond Order
ptC	planar tetracoordinate carbon
WBI	Wiberg Bond Index

References

1. Kealy, T.J.; Pauson, P.L. A New Type of Organo-Iron Compound. *Nature* **1951**, *168*, 1039–1040. doi: 10.1038/1681039b0. [CrossRef]
2. Wilkinson, G.; Rosenblum, M.; Whiting, M.C.; Woodward, R.B. The Structure of Iron Bis-Cyclopentadienyl. *J. Am. Chem. Soc.* **1952**, *74*, 2125–2126. doi: 10.1021/ja01128a527. [CrossRef]
3. Fischer, E.O.; Pfab, W. Cyclopentadien-Metallkomplexe, Ein Neuer Typ Metallorganischer Verbindungen. *Z. Naturforschg B* **1952**, *7*, 377–379. doi: 10.1515/znb-1952-0701. [CrossRef]
4. Pfab, W.; Fischer, E.O. Zur Kristallstruktur der Di-cyclopentadienyl-Verbindungen des Zweiwertigen Eisens, Kobalts und Nickels. *Z. Anorg. Allg. Chem.* **1953**, *274*, 316–322. doi: 10.1002/zaac.19532740603. [CrossRef]
5. Werner, H. At Least 60 Years of Ferrocene: The Discovery and Rediscovery of the Sandwich Complexes. *Angew. Chem. Int. Ed.* **2012**, *51*, 6052–6058. doi: 10.1002/anie.201201598. [CrossRef]
6. Mohammadi, N.; Ganesan, A.; Chantler, C.T.; Wang, F. Differentiation of Ferrocene D_{5d} and D_{5h} Conformers Using IR Spectroscopy. *J. Organomet. Chem.* **2012**, *713*, 51–59. doi: 10.1016/j.jorganchem.2012.04.009. [CrossRef]
7. Walawalkar, M.G.; Pandey, P.; Murugavel, R. The Redox Journey of Iconic Ferrocene: Ferrocenium Dications and Ferrocenate Anions. *Angew. Chem. Int. Ed.* **2021**, *60*, 12632–12635. [CrossRef]
8. Astruc, D. Why is Ferrocene so Exceptional? *Eur. J. Inorg. Chem.* **2017**, *2017*, 6–29. [CrossRef]
9. Malischewski, M.; Adelhardt, M.; Sutter, J.; Meyer, K.; Seppelt, K. Isolation and Structural and Electronic Characterization of Salts of the Decamethylferrocene Dication. *Science* **2016**, *353*, 678–682. doi: 10.1126/science.aaf6362. [CrossRef]
10. Hoffmann, R.; Alder, R.W.; Wilcox, C.F. Planar Tetracoordinate Carbon. *J. Am. Chem. Soc.* **1970**, *92*, 4992–4993. doi: 10.1021/ja00719a044. [CrossRef]
11. Yang, L.M.; Ganz, E.; Chen, Z.; Wang, Z.X.; Schleyer, P.V.R. Four Decades of the Chemistry of Planar Hypercoordinate Compounds. *Angew. Chem. Int. Ed.* **2015**, *54*, 9468–9501. [CrossRef] [PubMed]
12. Yañez, O.; Vásquez-Espinal, A.; Báez-Grez, R.; Rabanal-León, W.A.; Osorio, E.; Ruiz, L.; Tiznado, W. Carbon rings decorated with group 14 elements: New aromatic clusters containing planar tetracoordinate carbon. *New J. Chem.* **2019**, *43*, 6781–6785.
13. Raghunathan, S.; Yadav, K.; Rojisha, V.C.; Jaganade, T.; Prathyusha, V.; Bikkina, S.; Lourderaj, U.; Priyakumar, U.D. Transition between [R]- and [S]-stereoisomers without bond breaking. *Phys. Chem. Chem. Phys.* **2020**, *22*, 14983–14991. [CrossRef] [PubMed]
14. Zheng, H.F.; Yu, S.; Hu, T.D.; Xu, J.; Ding, Y.H. CAl_3X (X = B/Al/Ga/In/Tl) with 16 valence electrons: can planar tetracoordinate carbon be stable? *Phys. Chem. Chem. Phys.* **2018**, *20*, 26266–26272. [CrossRef]
15. Job, N.; Khatun, M.; Thirumoorthy, K.; CH, S.S.R.; Chandrasekaran, V.; Anoop, A.; Thimmakondu, V.S. $CAl_4Mg^{0/-}$: Global Minima with a Planar Tetracoordinate Carbon Atom. *Atoms* **2021**, *9*, 24. doi: 10.3390/atoms9020024. [CrossRef]
16. Das, P.; Chattaraj, P.K. $CSiGaAl_2^{-/0}$ and $CGeGaAl_2^{-/0}$ Having Planar Tetracoordinate Carbon Atoms in Their Global Minimum Energy Structures. *J. Comput. Chem.* **2022**, *43*, 894–905. [CrossRef] [PubMed]
17. Merino, G.; Méndez-Rojas, M.A.; Beltrán, H.I.; Corminboeuf, C.; Heine, T.; Vela, A. Theoretical Analysis of the Smallest Carbon Cluster Containing a Planar Tetracoordinate Carbon. *J. Am. Chem. Soc.* **2004**, *126*, 16160–16169. [CrossRef]
18. Wu, Y.B.; Li, Z.X.; Pu, X.H.; Wang, Z.X. Design of Molecular Chains Based on the Planar Tetracoordinate Carbon Unit C_2Al_4. *J. Phys. Chem. C* **2011**, *115*, 13187–13192. [CrossRef]
19. Suresh, C.H.; Frenking, G. Direct 1-3 Metal-Carbon Bonding and Planar Tetracoordinated Carbon in Group 6 Metallacyclobutadienes. *Organometallics* **2010**, *29*, 4766–4769. [CrossRef]
20. Zhang, C.; Wang, P.; Liang, J.; Jia, W.; Cao, Z. Theoretical study on a family of organic molecules with planar tetracoordinate carbon. *J. Mol. Struct. THEOCHEM* **2010**, *941*, 41–46. [CrossRef]
21. Thirumoorthy, K.; Karton, A.; Thimmakondu, V.S. From High-Energy C_7H_2 Isomers with A Planar Tetracoordinate Carbon Atom to An Experimentally Known Carbene. *J. Phys. Chem. A* **2018**, *122*, 9054–9064. doi: 10.1021/acs.jpca.8b08809. [CrossRef]
22. Guo, J.; Chai, H.; Duan, Q.; Qin, J.; Shen, X.; Jiang, D.; Hou, J.; Yan, B.; Li, Z.; Gu, F.; et al. Planar Tetracoordinate Carbon Species CLi_3E with 12-valence-electrons. *Phys. Chem. Chem. Phys.* **2016**, *18*, 4589–4593. doi: 10.1039/C5CP06081H. [CrossRef] [PubMed]

23. Wu, Y.B.; Jiang, J.L.; Lu, H.G.; Wang, Z.X.; Perez-Peralta, N.; Islas, R.; Contreras, M.; Merino, G.; Wu, J.I.; Schleyer, P.V.R. Starlike Aluminum Carbon Aromatic Species. *Chem. Eur. J.* **2011**, *17*, 714–719. [CrossRef] [PubMed]
24. Thirumoorthy, K.; Thimmakondu, V.S. Flat Crown Ethers with Planar Tetracoordinate Carbon Atoms. *Int. J. Quantum Chem.* **2021**, *121*, e26479. [CrossRef]
25. Guo, J.C.; Wu, H.X.; Ren, G.M.; Miao, C.Q.; Li, Y.X. D_{3h} $X_3Li_3^+$ (X=C, Si and Ge): Superalkali cations containing three planar tetracoordinate X atoms. *Comput. Theor. Chem.* **2016**, *1083*, 1–6. doi: 10.1016/j.comptc.2016.03.007. [CrossRef]
26. Thimmakondu, V.S.; Thirumoorthy, K. $Si_3C_2H_2$ Isomers with A Planar Tetracoordinate Carbon or Silicon Atom(s). *Comput. Theor. Chem.* **2019**, *1157*, 40–46. doi: 10.1016/j.comptc.2019.04.009. [CrossRef]
27. Thirumoorthy, K.; Cooksy, A.L.; Thimmakondu, V.S. $Si_2C_5H_2$ Isomers - Search Algorithms versus Chemical Intuition. *Phys. Chem. Chem. Phys.* **2020**, *22*, 5865–5872. [CrossRef]
28. Das, P.; Chattaraj, P.K. In Silico Studies on Selected Neutral Molecules, CGa_2Ge_2, $CAlGaGe_2$, and $CSiGa_2Ge$ Containing Planar Tetracoordinate Carbon. *Atoms* **2021**, *9*, 65. [CrossRef]
29. Wang, M.H.; Orozco-Ic, M.; Leyva-Parra, L.; Tiznado, W.; Barroso, J.; Ding, Y.H.; Cui, Z.H.; Merino, G. Planar Tetracoordinate Carbons in Allene-Type Structures. *J. Phys. Chem. A* **2021**, *125*, 3009–3014. doi: 10.1021/acs.jpca.1c02002. [CrossRef]
30. Das, P.; Khatun, M.; Anoop, A.; Chattaraj, P.K. $CSi_nGe_{4-n}^{2+}$ (n = 1–3): Prospective Systems Containing Planar Tetracoordinate Carbon (ptC). *Phys. Chem. Chem. Phys.* **2022**, *24*, 16701–16711. doi: 10.1039/D2CP01494G. [CrossRef]
31. Pancharatna, P.D.; Méndez-Rojas, M.A.; Merino, G.; Vela, A.; Hoffmann, R. Planar Tetracoordinate Carbon in Extended Systems. *J. Am. Chem. Soc.* **2004**, *126*, 15309–15315. [CrossRef] [PubMed]
32. Collins, J.B.; Dill, J.D.; Jemmis, E.D.; Apeloig, Y.; Schleyer, P.V.R.; Seeger, R.; Pople, J.A. Stabilization of Planar Tetracoordinate Carbon. *J. Am. Chem. Soc.* **1976**, *98*, 5419–5427. [CrossRef]
33. Li, X.; Zhang, H.F.; Wang, L.S.; Geske, G.; Boldyrev, A. Pentaatomic Tetracoordinate Planar Carbon, $[CAl_4]^{2-}$: A New Structural Unit and Its Salt Complexes. *Angew. Chem. Int. Ed.* **2000**, *39*, 3630–3632. [CrossRef]
34. Xu, J.; Zhang, X.; Yu, S.; Ding, Y.H.; Bowen, K.H. Identifying the Hydrogenated Planar Tetracoordinate Carbon: A Combined Experimental and Theoretical Study of CAl_4H and CAl_4H^-. *J. Phys. Chem. Lett.* **2017**, *8*, 2263–2267. [CrossRef]
35. Röttger, D.; Erker, G. Compounds Containing Planar-Tetracoordinate Carbon. *Angew. Chem. Int. Ed. Engl.* **1997**, *36*, 812–827. [CrossRef]
36. Li, X.; Zhai, H.J.; Wang, L.S. Photoelectron Spectroscopy of Pentaatomic Tetracoordinate Planar Carbon Molecules: CAl_3Si^- and CAl_3Ge^-. *Chem. Phys. Lett.* **2002**, *357*, 415–419. [CrossRef]
37. Zhang, C.J.; Wang, P.; Xu, X.L.; Xu, H.G.; Zheng, W.J. Photoelectron Spectroscopy and Theoretical Study of $Al_nC_5^{-/0}$ (n = 1–5) Clusters: Structural Evolution, Relative Stability of Star-Like Clusters, and Planar Tetracoordinate Carbon Structures. *Phys. Chem. Chem. Phys.* **2021**, *23*, 1967–1975. [CrossRef]
38. Tal'rose, V.L.; Lyubimova, A.K. Secondary Processes in the Ion Source of the Mass Spectrometer. *Dokl. Akad. Nauk SSSR* **1952**, *86*, 909–912.
39. Yamashita, M.; Yamamoto, Y.; Akiba, K.Y.; Hashizume, D.; Iwasaki, F.; Takagi, N.; Nagase, S. Syntheses and Structures of Hypervalent Pentacoordinate Carbon and Boron Compounds Bearing an Anthracene Skeleton-Elucidation of Hypervalent Interaction Based on X-ray Analysis and DFT Calculation. *J. Am. Chem. Soc.* **2005**, *127*, 4354. [CrossRef]
40. Fernández, I.; Uggerud, E.; Frenking, G. Stable Pentacoordinate Carbocations: Structure and Bonding. *Chem. Eur. J.* **2007**, *13*, 8620–8626. [CrossRef]
41. Yamaguchi, T.; Yamamoto, Y.; Kinoshita, D.; Akiba, K.Y.; Zhang, Y.; Reed, C.A.; Hashizume, D.; Iwasaki, F. Synthesis and Structure of a Hexacoordinate Carbon Compound. *J. Am. Chem. Soc.* **2008**, *130*, 6894–6895. [CrossRef] [PubMed]
42. Vassilev-Galindo, V.; Pan, S.; Donald, J.K.; Merino, G. Planar Pentacoordinate Carbons. *Nat. Chem. Rev.* **2018**, *2*, 0114. [CrossRef]
43. White, E.T.; Tang, J.; Oka, T. CH_5^+: The Infrared Spectrum Observed. *Science* **1999**, *284*, 135–137. [CrossRef] [PubMed]
44. Schleyer, P.v.R.; Würthwein, E.U.; Kaufmann, E.; Clark, T.; Pople, J.A. Effectively Hypervalent Molecules. 2. Lithium Carbide (CLi_5), Lithium Carbide (CLi_6), and the Related Effectively Hypervalent First Row Molecules, CLi_5-nHn and CLi_6-nHn. *J. Am. Chem. Soc.* **1983**, *105*, 5930. [CrossRef]
45. McKee, W.C.; Agarwal, J.; Schaefer, H.F., III; Schleyer, P.V.R. Covalent Hypercoordination: Can Carbon Bind Five Methyl Ligands? *Angew. Chem. Int. Ed.* **2014**, *53*, 7875–7878. [CrossRef]
46. Scherbaum, F.; Grohmann, A.; Müller, G.; Schmidbaur, H. Synthesis, Structure, and Bonding of the Cation $[(C_6H_5)_3PAu_5C]^{\oplus}$. *Angew. Chem. Int. Ed.* **1989**, *28*, 463–465. doi: 10.1002/anie.198904631. [CrossRef]
47. Dávalos, J.A.; Herrero, R.; Abboud, J.L.M.; Mó, O.; Yáñez, M. How Can a Carbon Atom Be Covalently Bound to Five Ligands? The Case of $Si_2(CH_3)_7^+$. *Angew. Chem. Int. Ed.* **2007**, *46*, 381. [CrossRef]
48. Kudo, H. Observation of Hypervalent CLi_6 by Knudsen-Effusion Mass Spectrometry. *Nature* **1992**, *355*, 432. [CrossRef]
49. Scherbaum, F.; Grohmann, A.; Huber, B.; Krüger, C.; Schmidbaur, H. Aurophilicity as a Consequence of Relativistic Effects:The Hexakis(triphenylphosphaneaurio)methane Dication $[(Ph_3PAu)_6C]^{2\oplus}$. *Angew. Chem. Int. Ed.* **1988**, *27*, 1544–1546. doi: 10.1002/anie.198815441. [CrossRef]
50. Hogeveen, H.; Kwant, P. Direct Observation of a Remarkably Stable Dication of Unusual Structure: $(CCH_3)_6^{2+}$. *Tetrahedron Lett.* **1973**, *14*, 1665–1670. doi: 10.1016/S0040-4039(01)96023-X. [CrossRef]
51. Malischewski, M.; Seppelt, K. Crystal Structure Determination of the Pentagonal-Pyramidal Hexamethylbenzene Dication $C_6(CH_3)_6^{2+}$. *Angew. Chem. Int. Ed.* **2017**, *56*, 368–370. doi: 10.1002/anie.201608795. [CrossRef] [PubMed]

52. Olah, G.A.; Rasul, G. Triprotonated Methane, CH_7^{3+}: The Parent Heptacoordinate Carbonium Ion. *J. Am. Chem. Soc.* **1996**, *118*, 8503–8504. doi: 10.1021/ja961081v. [CrossRef]
53. Gao, Y.; Shao, N.; Zhou, R.; Zhang, G.; Zeng, X.C. [CTi_7^{2+}]: Heptacoordinate Carbon Motif? *J. Phys. Chem. Lett.* **2012**, *3*, 2264–2268. doi: 10.1021/jz300859t. [CrossRef] [PubMed]
54. Wang, G.; Rahman, A.K.F.; Wang, B. Ab Initio Calculations of Ionic Hydrocarbon Compounds with Heptacoordinate Carbon. *J. Mol. Model.* **2018**, *24*, 116. [CrossRef] [PubMed]
55. Wang, Y.; Huang, Y.; Yin, B.; Yang, B.; Liu, R. Octacoordinate Carbons Encaged Inside Carborane Clusters: A Density Functional Theory Investigation. *J. Phys. Chem. A* **2008**, *112*, 7643–7651. doi: 10.1021/jp801332b. [CrossRef]
56. Guo, J.C.; Feng, L.Y.; Dong, C.; Zhai, H.J. A Designer 32-Electron Superatomic CBe_8H_{12} Cluster: Core-shell Geometry, Octacoordinate Carbon, and Cubic Aromaticity. *New J. Chem.* **2020**, *44*, 7286–7292. doi: 10.1039/D0NJ00778A. [CrossRef]
57. Yang, L.M.; Ding, Y.H.; Sun, C.C. Design of Sandwichlike Complexes Based on the Planar Tetracoordinate Carbon Unit CAl_4^{2-}. *J. Am. Chem. Soc.* **2007**, *129*, 658–665. [CrossRef]
58. Yang, L.m.; Ding, Y.h.; Sun, C.c. Assembly and Stabilization of a Planar Tetracoordinated Carbon Radical CAl_3Si: A Way To Design Spin-Based Molecular Materials. *J. Am. Chem. Soc.* **2007**, *129*, 1900–1901. [CrossRef]
59. Luo, Q.; Zhang, X.H.; Huang, K.L.; Liu, S.Q.; Yu, Z.H.; Li, Q.S. Theoretical Studies on Novel Main Group Metallocene-like Complexes Involving Planar Hexacoordinate Carbon η^6-$B_6C_2^-$ Ligand. *J. Phys. Chem. A* **2007**, *111*, 2930–2934. [CrossRef]
60. Li, S.D.; Miao, C.Q.; Ren, G.M.; Guo, J.C. Triple-Decker Transition-Metal Complexes (CnHn)M(B6C)M(CnHn) (M = Fe, Ru, Mn, Re; n = 5, 6) Containing Planar Hexacoordinate Carbon Atoms. *Eur. J. Inorg. Chem.* **2006**, *2006*, 2567–2571. [CrossRef]
61. Yañez, O.; Vásquez-Espinal, A.; Pino-Rios, R.; Ferraro, F.; Pan, S.; Osorio, E.; Merino, G.; Tiznado, W. Exploiting Electronic Strategies to Stabilize A Planar Tetracoordinate Carbon in Cyclic Aromatic Hydrocarbons. *Chem. Commun.* **2017**, *53*, 12112–12115. doi: 10.1039/C7CC06248F. [CrossRef]
62. Thirumoorthy, K.; Chandrasekaran, V.; Cooksy, A.L.; Thimmakondu, V.S. Kinetic Stability of $Si_2C_5H_2$ Isomer with a Planar Tetracoordinate Carbon Atom. *Chemistry* **2021**, *3*, 13–27. [CrossRef]
63. Weigend, F.; Ahlrichs, R. Balanced Basis Sets of Split Valence, Triple Zeta Valence and Quadruple Zeta Valence Quality for H to Rn: Design and Assessment of Accuracy. *Phys. Chem. Chem. Phys.* **2005**, *7*, 3297–3305. [CrossRef]
64. Lee, C.; Yang, W.; Parr, R.G. Development of the Colle-Salvetti Correlation-Energy Formula Into a Functional of the Electron Density. *Phys. Rev. B* **1988**, *37*, 785–789. doi: 10.1103/PhysRevB.37.785. [CrossRef]
65. Tao, J.; Perdew, J.P.; Staroverov, V.N.; Scuseria, G.E. Climbing the Density Functional Ladder: Nonempirical Meta–Generalized Gradient Approximation Designed for Molecules and Solids. *Phys. Rev. Lett.* **2003**, *91*, 146401. [CrossRef]
66. Zhao, Y.; Truhlar, D.G. A New Local Density Functional for Main-Group Thermochemistry, Transition Metal Bonding, Thermochemical Kinetics, and Noncovalent Interactions. *J. Chem. Phys.* **2006**, *125*, 194101. [CrossRef] [PubMed]
67. Chai, J.D.; Head-Gordon, M. Long-Range Corrected Hybrid Density Functionals with Damped Atom-Atom Dispersion Corrections. *Phys. Chem. Chem. Phys.* **2008**, *10*, 6615–6620. [CrossRef]
68. Grimme, S.; Antony, J.; Ehrlich, S.; Krieg, H. A Consistent and Accurate Ab Initio Parametrization of Density Functional Dispersion Correction (DFT-D) for the 94 Elements H-Pu. *J. Chem. Phys.* **2010**, *132*, 154104. [CrossRef]
69. Becke, A.D.; Johnson, E.R. Exchange-Hole Dipole Moment and the Dispersion Interaction. *J. Chem. Phys.* **2005**, *122*, 154104. [CrossRef]
70. Grimme, S.; Ehrlich, S.; Goerigk, L. Effect of the Damping Function in Dispersion Corrected Density Functional Theory. *J. Comput. Chem.* **2011**, *32*, 1456–1465. [CrossRef]
71. Glendening, E.D.; Weinhold, F. Natural Resonance Theory: I. General Formalism. *J. Comput. Chem.* **1998**, *19*, 593–609. [CrossRef]
72. Schlegel, H.B.; Millam, J.M.; Iyengar, S.S.; Voth, G.A.; Daniels, A.D.; Scuseria, G.E.; Frisch, M.J. Ab Initio Molecular Dynamics: Propagating the Density Matrix with Gaussian Orbitals. *J. Chem. Phys.* **2001**, *114*, 9758–9763. [CrossRef]
73. Frisch, M.J.; Trucks, G.W.; Schlegel, H.B.; Scuseria, G.E.; Robb, M.A.; Cheeseman, J.R.; Scalmani, G.; Barone, V.; Petersson, G.A.; Nakatsuji, H.; et al. *Gaussian 16 Revision B.01*; Gaussian Inc.: Wallingford, CT, USA, 2016.
74. Coriani, S.; Haaland, A.; Helgaker, T.; Jørgensen, P. The Equilibrium Structure of Ferrocene. *ChemPhysChem* **2006**, *7*, 245–249. [CrossRef] [PubMed]
75. Zhang, Y.; Xu, X.; Goddard, W.A. Doubly Hybrid Density Functional for Accurate Descriptions of Nonbond Interactions, Thermochemistry, and Thermochemical Kinetics. *Proc. Natl. Acad. Sci. USA* **2009**, *106*, 4963–4968. [CrossRef]
76. Zhang, I.Y.; Wu, J.; Xu, X. Extending the Reliability and Applicability of B3LYP. *Chem. Commun.* **2010**, *46*, 3057–3070. [CrossRef]
77. Seiler, P.; Dunitz, J.D. Low-Temperature Crystallization of Orthorhombic Ferrocene: Structure Analysis at 98 K. *Acta Cryst. B* **1982**, *38*, 1741–1745. [CrossRef]
78. Zubarev, D.Y.; Boldyrev, A.I. Developing Paradigms of Chemical Bonding: Adaptive Natural Density Partitioning. *Phys. Chem. Chem. Phys.* **2008**, *10*, 5207–5217. [CrossRef] [PubMed]
79. Zubarev, D.Y.; Boldyrev, A.I. Revealing Intuitively Assessable Chemical Bonding Patterns in Organic Aromatic Molecules via Adaptive Natural Density Partitioning. *J. Org. Chem.* **2008**, *73*, 9251–9258. [CrossRef]
80. Lu, T.; Chen, F. Multiwfn: A Multifunctional Wavefunction Analyzer. *J. Comput. Chem.* **2012**, *33*, 580–592. [CrossRef]